Unconventional Morphologies of Symmetric, Diblock Copolymers Due to Film Thickness Constraints

T. P. Russell,* A. Menelle, and S. H. Anastasiadis

IBM Research Division, Almaden Research Center, 650 Harry Road, San Jose, California 95120-6099

S. K. Satija and C. F. Majkrzak

Reactor Radiation Division, National Institute of Standards and Technology, Gaithersburg, Maryland 20899

Received April 1, 1991; Revised Manuscript Received June 18, 1991

ABSTRACT: The morphology of thin films of symmetric, diblock copolymers of polystyrene (PS) and poly(methyl methacrylate) (PMMA) has been investigated as a function of film thickness where the total thickness of the films was less than or equal to $3L/2$ where L is the period of the lamellar microdomain in the bulk. In all cases, a layered, lamellar morphology oriented parallel to the surface of the film was found. However, the thicknesses of the PS and PMMA layers and the width of the interface between the layers were found to vary with film thickness. Finally, in the case of a film with a thickness of L, a phase-mixed morphology on top of underlying layers of PS and PMMA was found, demonstrating a marked perturbation on the morphology of the diblock copolymer in this upper layer from that seen usually in thin multilayer films and in the bulk. The results from these studies were found to be in agreement with X-ray reflectivity and X-ray photoelectron spectroscopy studies.

Introduction

The morphology of an A–B diblock copolymer in the bulk is defined by the molecular weights of the blocks comprising the copolymer, N_A and N_B, and the segmental interaction parameter, χ_{AB}, between the different components. For values of $\chi_{AB}N$ greater than the spinodal value, morphologies ranging from spheres to cylinders to bicontinuous phases to lamellae can be found depending upon the volume fraction of A and B in the copolymer.[1-8] Theoretically the nature of the morphology of diblock copolymers has been treated with reasonable success in predicting the observed morphology.[10-15] In the vicinity of an interface, specific interactions of one of the components with the surface can induce ordering of the diblock copolymer above the order/disorder transition temperature[16] and will cause a preferential segregation of one of the components to the interface.[17-20] At temperatures below the order/disorder transition temperature the preferential interaction of one of the blocks with the substrate interface or air interface causes an orientation of the domains with respect to the surface.[21-30]

Thin films of diblock copolymers represent a situation where the copolymer experiences restraints induced by the proximity of two interfaces, these being the air/copolymer and copolymer/substrate interfaces. In addition to the preferential segregation of specific blocks to the two interfaces, the copolymer faces the restraint of a hard barrier, namely, the substrate, and the surface energies at the free surface. In thin films of diblock copolymers, where the film thickness is several times the characteristic period of the copolymer in the bulk, the microphases are highly oriented with respect to the substrate plane. This has been shown for lamellar and cylindrical microdomain morphologies by neutron reflectivity,[16,25] dynamic secondary ion mass spectroscopy,[26,27] and optical microscopy[21-23,26,28,29] and for spherical, cylindrical, and lamellar morphologies by transmission electron microscopy.[30] In general, the film thickness will not be precisely a given number of periods and, consequently, to accommodate the oriented microphase-separated morphology, at the free surface terraces, islands, or holes form where the height of each step in the topography is given by 1 period of the copolymer morphology.[21-23,26,28-30] Thus, the thickness is quantized in terms of the morphology.

Decreasing the thickness of the film such that it approaches or is less than 1 period in thickness places further restraints on the copolymer molecules. Henkee et al.[30] report that, in this case, the normal microdomain morphology is inhibited, but, with electron microscopy, it was difficult to assess the precise nature of the morphology. That is to say, the components may be phase mixed where the ordering process is suppressed, or the microphase separation could be such that it is on a smaller scale. It is the intent of this article to address this question using neutron reflectivity on thin films of symmetric diblock copolymers of polystyrene (PS) and poly(methyl methacrylate) (PMMA) denoted P(d-S-*b*-MMA) where the styrene block is perdeuterated.

For P(S-*b*-MMA) it has been shown that thin films of the symmetric diblock copolymers form a multilayered morphology.[16,25] Specific interactions of the PMMA block with the substrate (in this case Si or SiO_2) and the lower surface energy of PS cause a preferential segregation of PMMA to the substrate and PS to the air interface. Neutron reflectivity studies have, also, shown that the thicknesses of the lamellar layers at both interfaces are precisely half the thickness of the respective layers in the bulk of the film.[16,25] Consequently, the thickness of the thin films at any point on the specimen is given by $(n + 1/2)L$ where n is an integer and L is the period of the lamellar microdomain morphology in the bulk. The question that this article addresses is the morphology in films with a thickness less than $3L/2$. It is shown that regardless of the film thickness the films are always microphase separated. However, the characteristics of the morphology can differ substantially from those of bulk films. In particular, both the period and the interphase thickness are modified in order to accommodate the restraints placed on the morphology by the film thickness.

0024-9297/91/2224-6263$02.50/0

Table I
Sample Thicknesses

label	desired thickness,[a] Å	thickness measd by: ellipsometry, Å	X-ray reflectivity, Å	neutron reflectivity, Å
$L/4$	190	188	215	209
$L/2$	381	400	406	381
$3L/4$	571	568	602	555
L	762	734	740	726
$3L/2$	1143	1320	1365	1299

[a] The long period of the lamellar microdomain morphology in the bulk specimens and in ordered multilayers is 762 Å for the copolymer used in this study.

Experimental Section

A symmetric, diblock copolymer of PS and PMMA where the PS block was perdeuterated was used in this study. This is denoted as P(d-S-*b*-MMA). The PS block had a molecular weight of 169 500, and that of the PMMA block was 131 900 where the weight- to number-average molecular weight of the copolymer was 1.08. In terms of segments there were 1513 styrene segments and 1319 methyl methacrylate segments, which yields a fraction of PS segments of 0.53. The copolymer was purchased from Polymer Laboratories and was purified by successive extractions in cyclohexane. This treatment removes the unreacted PS homopolymer from the copolymer.

Specimens from the neutron reflectivity studies were prepared by spin-casting films onto Si substrates at a speed of 2×10^3 rpm from toluene solutions. The thickness of the films was varied by altering the concentration of the casting solutions. All films were annealed for 240 h at 170 °C to ensure that the films had achieved thermal equilibrium. The Si substrates were 10 cm in diameter polished to $\lambda/4$, where $\lambda = 4300$ Å, with the (100) crystal face on the surface. To ensure that the substrate did not bow during the experiment, substrates with a thickness of 5 mm were used. The high optical reflectivity of the Si permitted an easy means by which the quality of the specimen could be assessed during the preparation simply by the examination of the uniformity of the interference colors.

Neutron reflectivity measurements were performed on the BT-4 triple-axis diffractometer at the reactor experimental hall of the National Institute of Standards and Technology. The experimental geometry has been described elsewhere[25] and will only be briefly outlined here. A collimated beam of neutrons with a wavelength, λ, of 2.35 Å, $\Delta\lambda/\lambda = 0.02$, and an angular divergence of 0.02° illuminated the specimen at glancing angles. An ^{3}He-filled gas detector located after a 2-mm cadmium receiving slit (330 mm after the specimen) was used to measure both the incident and reflected beams. Reflectivity profiles were obtained with the specimen (oriented vertically) rotating at an angle θ and the detector at an angle 2θ, keeping the diffraction vector oriented normal to the sample surface. The background was measured with the detector offset by +0.6° from the specular position and performing the normal θ–2θ scan.

Results and Discussion

Films having five different thicknesses were investigated in this study. In particular, films with approximate thicknesses of $L/4$, $L/2$, $3L/4$, L, and $3L/2$ were prepared where L is the period of the lamellar microdomain morphology in the bulk. For the P(d-S-*b*-MMA) of interest here, $L = 762$ Å.[25] The film thicknesses determined from optical ellipsometry measurements are shown in Table I, and, as can be seen, the thicknesses correspond well to the desired values. Preparing films with the exact thicknesses is most difficult since slight changes in the concentration and spinning speed will cause changes in the film thickness. These thicknesses are, however, suitable for the studies here.

An alternate means by which the film thickness can be determined is by X-ray reflectivity. While there is an electron density difference between PS and PMMA, this difference is much smaller than that between the copolymer and Si. Consequently, the reflection coefficients at the air/P(d-S-*b*-MMA) and the P(d-S-*b*-MMA)/Si will dominate the X-ray reflectivity measurements. As a very good, first approximation the X-ray measurements will be characteristic of a uniform polymer film on an Si substrate. Details concerning the internal structure of the copolymer are not easily observed by the X-ray measurements whereas roughness at the air/P(d-S-*b*-MMA) and P(d-S-*b*-MMA)/Si interfaces will be easily detected.

Table II
X-ray Photoelectron Spectroscopy Results

specimen	ϕ^S_{PS}[a]	specimen	ϕ^S_{PS}[a]
$L/4$	1.0	L	0.54
$L/2$	1.0	$3L/2$	1.0
$3L/4$	1.0		

[a] ϕ^S_{PS} is the surface composition of d-PS at the air/polymer interface, integrated over the first ~75 Å of the specimen. It should be noted that angular-dependent studies showed no composition dependence as a function of depth.

X-ray reflectivity measurements on all five specimens yielded relatively simple profiles with oscillations characteristic of only the film thickness. The oscillations were evident up to $k_{z,0} = (2\pi/\lambda) \sin\theta$ of ~0.15 Å^{-1} where λ is the wavelength and θ is the grazing angle of incidence. The subscripts denote that the scattering vector is in the z-direction, i.e., normal to the surface, and it is the value in vacuo (medium 0). Roughness at both the air/P(d-S-*b*-MMA) and P(d-S-*b*-MMA)/Si interfaces were ~6 Å assuming a Gaussian distribution of deviations about a mean value. The thicknesses determined from the X-ray reflectivity measurements are shown in Table I also. The agreement between the ellipsometric measurements and the X-ray reflectivity measurements is quite good in most cases. In those cases where deviations are evident, differences in the positions on the specimen where the measurements are made can be the source of the discrepancy. Ellipsometry measures only one point on the specimen whereas the X-ray measurements are taken on a thin line that extends the length of the specimen. Nonetheless, the values agree with one another to within 10%.

Prior to discussing the details of the neutron reflectivity measurements, it is worthwhile to present the results of X-ray photoelectron spectroscopy (XPS) studies on these films. The results of the XPS measurements are shown in Table II. The O_{1s} and C_{1s} signals serve as signatures for the PMMA and PS portions of the diblock copolymer, permitting the evaluation of the relative concentrations of both components as a function of depth over the first 75 Å from the air/copolymer interface.[17,31] No variation in the concentration of either component as a function of depth was found. The results of the XPS studies show that for all the sample thicknesses studied, with the exception of the specimen with a thickness of L, only PS was observed in the first 75 Å from the film surface. This result alone states that the copolymer films are microphase separated. For the L-thick specimen the volume fraction of PS at the surface was found to be 0.54. This corresponds to the composition of PS in the diblock copolymer and indicates that, at the surface, the copolymer is phase mixed. Consequently, prior to the use of any modeling, which is necessary for the neutron reflectivity studies, XPS has provided some very important pieces of information to which the neutron reflectivity results must conform.

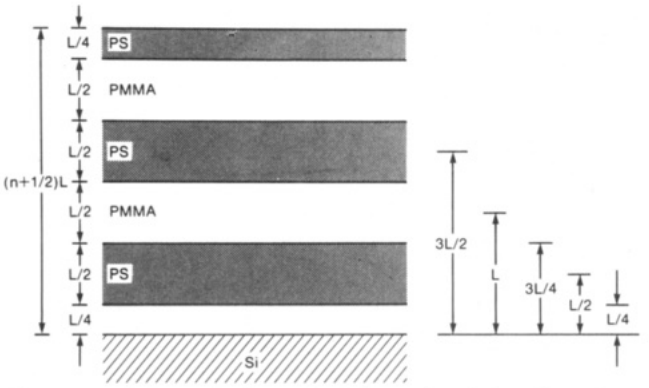

Figure 1. Schematic diagram of the ordered, lamellar microdomain morphology found in thin films of symmetric, diblock copolymers of P(S-*b*-MMA). Specific details can be found in ref 25. To the left are the thicknesses of the specimens investigated in this study.

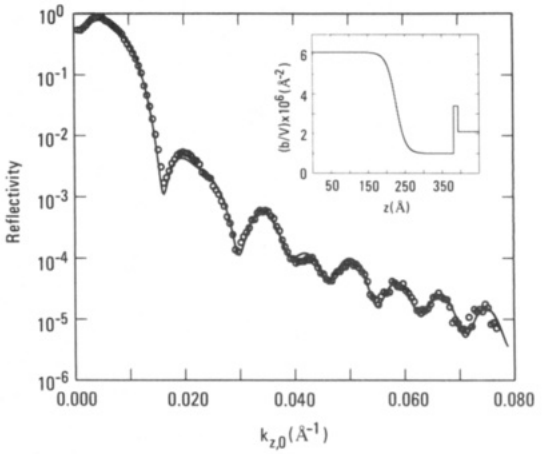

Figure 2. Neutron reflectivity profile for a P(d-S-*b*-MMA) specimen $L/2$ thick. The circles represent the measured data whereas the solid line was calculated by using the scattering length density profile shown in the inset. Zero in the inset indicates the air surface.

The morphology for thin films of diblock copolymers on silicon substrates as determined from previous dynamic secondary ion mass spectroscopy[26,27] and neutron reflectivity studies[16,25] is shown schematically in Figure 1. As mentioned in the introduction, the total thickness at any point in the specimen is given by $(n + 1/2)L$ where n is an integer and L is the period of the lamellar microdomain morphology in the bulk. Mismatches in the initial thickness of the specimen to $(n + 1/2)L$ result in the formation of islands, depressions, or terraces on the film surface. The films that have been prepared for this study, as evidenced by the ellipsometry and X-ray reflectivity measurements, correspond to those indicated on the right of the figure. Two thicknesses, namely $3L/2$ and $L/2$, correspond to cases where n is 1 and 0, respectively. Consequently, these films should yield reflectivity results, which are relatively easy and straightforward to interpret.

In general, neutron reflectivity is the optical transform of the variation in the scattering length density as a function of depth in the specimen. In only a few cases can one analytically calculate the reflectivity profile. Normally, one is forced into a situation where a model for the scattering length density variation as a function of depth is assumed, the reflectivity profile is then calculated and compared with the observed reflectivity profile. Detailed descriptions of the manner in which the reflectivity profiles are calculated have appeared elsewhere[32-37] and will not be repeated here. Suffice it to say that a scattering length density profile is assumed and is then divided into a histogram comprised of incremental changes in the scattering length density where the width of the layers defining the step changes in the scattering length density depends upon the detail required. For example, in a multilayered system coarse layer thicknesses are used to define each layer whereas small layer thicknesses (~5 Å) are used to define the scattering length density variation across the interface between the layers or at the air surface to define the surface roughness. While this method is approximate in defining the scattering length density profile, the reflectivity can be calculated exactly. Provided appropriate layer thicknesses are taken, this histogram provides a very good estimate of the real profile. It should be emphasized, though, that the models used to calculate the reflectivity profiles may not be unique. Given the nature of the films under consideration here, coupled with the independent XPS data, relatively simple models can be developed. While other models may also describe the reflectivity profiles, the models presented herein should be very close to an accurate description of the morphology in the films. In all cases the simplest model was taken as being the proper description of the morphology, thereby minimizing the number of adjustable parameters.

The neutron reflectivity profile for the $L/2$-thick specimen is shown in Figure 2. The reflectivity profile below $k_{z,0} \simeq 0.008$ exhibits total external reflection as would be expected since the scattering length density of the copolymer is positive, making the effective neutron refractive index slightly less than 1. The reduction in the reflectivity at smaller scattering vectors is simply a geometric effect. Since the size of the substrate and the incident neutron beam are finite, then, at small grazing angles of incidence, the specimen does not fully intercept the incident beam. Since the reflectivity is the ratio of the reflected to incident neutrons, this forces the measured reflectivity to decrease with decreasing angle. Above the critical angle, as $k_{z,0}$ increases, the reflectivity profile is seen to decrease rapidly down to $\sim 5 \times 10^{-6}$ at $k_{z,0} \simeq 0.078$. A series of oscillations are seen in the reflectivity profile which characterize both the total film thickness and the thickness of the d-PS layers at the surface. The scattering length density profile in the inset was used to calculate the reflectivity profile shown as the solid line in the figure. As can be seen, the agreement between the measured and calculated profiles is quite good over the entire $k_{z,0}$ range. The model basically consists of a 225-Å layer of d-PS on a 156-Å layer of PMMA with scattering length densities of 6.1×10^{-6} Å^{-2} and 1.0×10^{-6} Å^{-2}, respectively. These correspond to the scattering length densities of bulk d-PS and PMMA. Separating the two layers is an interface that could be described with a hyperbolic tangent function with an effective width, a_I, of 50 Å. The width of the interface is defined as the product of the inverse of the slope at the midway point in the gradient times the scattering length density difference between the layers.

This result is in agreement with previous X-ray scattering[38] and neutron reflectivity measurements[25] and shows that, for the $n = 0$ case, i.e., $L/2$, an unperturbed morphology is found. It should be noted that an oxide layer on the Si with a thickness of ~20 Å and a scattering length density of 3.48×10^{-6} Å^{-2} was necessary in order to yield agreement between the measured and calculated profiles. The substrates were cleaned by immersion in an acid bath, thoroughly rinsed with deionized water, placed in isopropyl alcohol vapors, and then dried prior to use. Consequently, the presence of the oxide layer is not surprising and, in fact, should be expected. For completeness, the scattering length density of the Si was taken

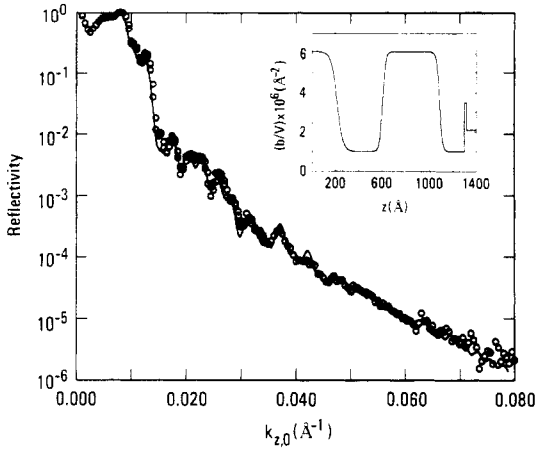

Figure 3. Neutron reflectivity profile for a P(d-S-*b*-MMA) film $3L/2$ thick. The circles represent the measured data whereas the solid line was calculated by using the scattering length density profile shown in the inset.

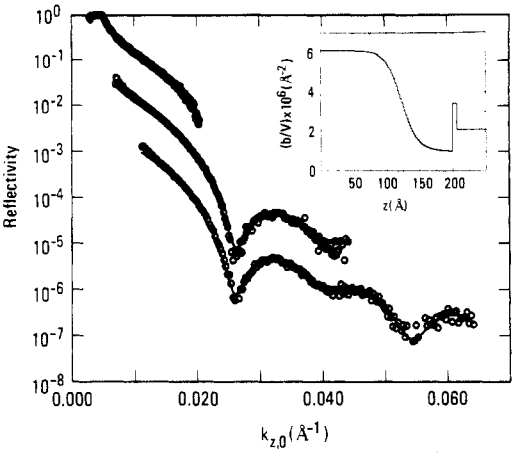

Figure 4. Neutron reflectivity profile for a P(d-S-*b*-MMA) film $L/4$ thick. The circles represent the measured data whereas the solid line was calculated by using the scattering length density profile shown in the inset. The three profiles were obtained on POSY-II at IPNS at three different angles of incidence. These were offset from one another by factors of 10. The variation in the resolution ($\Delta k/k$) for the different angles did not permit merging the data together. The calculated reflectivity profiles take into account the different values of $\Delta k/k$.

as $2.0.3 \times 10^{-6}$ Å^{-2} based on the density of Si and the tabulated value of the neutron scattering length of Si.[39]

In Figure 3 is shown the neutron reflectivity profile for a specimen that is slightly thicker than $3L/2$. Unlike the reflectivity profile for the $L/2$ specimen, the reflectivity profile above the critical angle exhibits a high-frequency oscillation characteristic of the total thickness of the specimen. These, however, are modulated by frequencies characteristic of the thickness of the layers formed in the multilayer structure of the copolymer. The solid line in Figure 3 is the reflectivity profile calculated by using the scattering length density profile shown in the inset. This profile is characterized by a layer of d-PS at the air surface with a thickness of 210 Å. This is in keeping with the XPS results discussed previously. Following this as one goes into the specimen are layers of PMMA, d-PS, and PMMA with thicknesses of 392, 483, and 214 Å, respectively.

As would be expected, the strong interactions of PMMA with the substrate result in a layer of pure PMMA at the Si or SiO_2 interface. The total thickness of the film is ~1300 Å, which is ~157 Å thicker than the ideal $3L/2$ film thickness of 1143 Å. This perturbation, in comparison to the results for the $L/2$ thick film, has resulted in a change in the copolymer morphology. For example, both the PMMA layer adjacent to the substrate and the adjoining d-PS layer are slightly thicker than the values one would expect from the $L/2$-thick specimen. In fact, on the basis of these results, a lamellar period of 856 Å would be predicted rather than the value of 762 Å found in previous studies. This represents nearly a 12% increase in the copolymer period induced by the restriction of the film thickness. This increase in the long period, despite the increase in the chain extension of the copolymer molecules at the interface and the increased number of junction points at the interface, does not give rise to a substantial increase in the interfacial width. Between the first three layers from the substrate, an interfacial width of 52 Å is found, which is only slightly greater than the value of 50 Å found typically of these copolymers. This increase is within the error limits of the reflectivity measurements. However, a surprising result is found for the interface between the d-PS layer at the air surface and the adjacent PMMA layer. Here, an interfacial width of 100 Å is found, which is well outside experimental errors. This result is even more surprising when one considers that the d-PS layer at the air surface is only slightly less than the value found for the $L/2$-thick specimen. It is apparent, however, that the forces exerted on the film are sufficient to induce this broadening.

A question immediately arises as to why the copolymer films have not formed islands on the surface of the film.[40] It has been shown in several studies that films with thicknesses not equal to $(n + 1/2)L$ form terraces on the surface with a step height equal to L, the period. In order for this to occur, one must consider the excess surface energy that is generated. If it is assumed that the islands would have an average diameter of $\bar{D}$, then the amount of surface energy required to form the islands is $N\pi\bar{D}L\sigma_E$ where N is the number of islands and σ_E the surface energy per unit area of d-PS. It should be noted that energy required to form islands depends on the molecular weight of the copolymer through L. Consequently, the higher the molecular weight, the more difficult it is to form islands. For the case studied here, it appears to be energetically more favorable to perturb the copolymer morphology rather than produce islands on the surface of the film.

The reflectivity profile for the $L/4$-thick specimen is shown in Figure 4. The data shown in this figure were obtained on POSY-II at the Argonne National Laboratory. POSY-II is a time-of-flight reflectometer which has been described in detail elsewhere.[36,37,41] The three separate reflectivity profiles were obtained at three different angles of incidence. Under the experimental conditions used, the resolution function of the reflectometer changed with incidence angle. Consequently, the data have not been merged together. The data have been offset by factors of 10 for clarity. Reflectivity profiles were calculated for each angular setting, taking into acount the different resolution functions.

The reflectivity profile is characterized by the total external reflection below the critical $k_{z,0} \sim 0.005$ Å^{-1}. The reflectivity then decreases, exhibiting a broad shoulder prior to the first minimum. This is then followed by a series of shallow maxima and minima. It is evident from a cursory examination of the reflectivity profile that there are at least two frequencies of oscillations in the profile. Consequently, without further analysis it is clear that the copolymer film is not phase mixed; i.e., the scattering length density as a function of depth is not constant. In fact, the solid line drawn through the experimental points was calculated by using the scattering length density profile

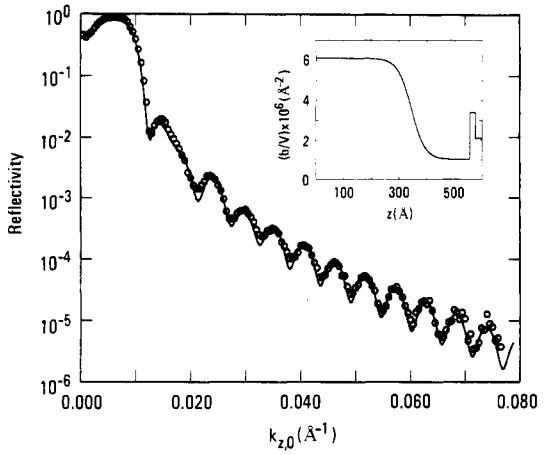

Figure 5. Neutron reflectivity profile for a film of P(d-S-*b*-MMA) that is $3L/4$ thick. The circles are the measured profile whereas the solid line was calculated by using the scattering length density profile shown in the inset.

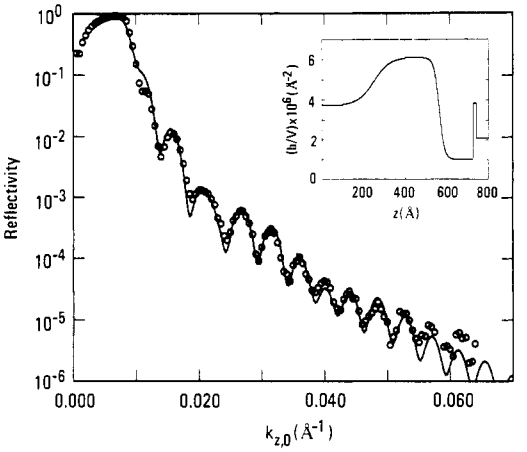

Figure 6. Neutron reflectivity profile for a film of P(d-S-*b*-MMA) that is L thick. The circles represent the measured profile whereas the solid line was calculated by using the scattering length density profile shown in the inset.

shown in the inset. The picture that emerges is relatively simple. At the air surface is a layer of pure d-PS with a thickness of 87 Å. Again, this is consistent with the XPS results, which showed that over the first 75 Å in the specimen only PS is seen at the air surface. This d-PS layer is on top of a 122-Å layer of PMMA. The PMMA, as in all other cases, would be expected at the substrate surface, which in this case is an ~10-Å layer of an oxide on top of the Si substrate. The two layers are separated by an interface with a width of 48 Å. The width is identical with that seen for the $L/2$-thick specimen despite the reduced thicknesses of the d-PS and PMMA layers. It is impossible, from the reflectivity results alone, to describe the exact condition of the copolymer chains. However, there are two possibilities. First, the average orientation of the chains remains normal to the film surface, and the extension of the molecules normal to the interface is reduced in comparison to that found in the $L/2$ case. Second, it is possible that the average extension of the molecules at the interface is maintained and the molecules, on average, are tilted away from the surface normal. Either is possible, and spectroscopic methods are required to distinguish these alternatives. Without question, though, the restraint imposed by the film thickness has induced a significant change in the morphology of the copolymer.

It is important, at this point, to note that a microphase-separated morphology was retained despite the confinement of the copolymer between the narrowly separated interfaces. The retention of the microphase separation is, more than likely, strongly biased by the preferential segregation of the PS to the air surfaces and PMMA to the substrate interface. If, for example, gold were used as a substrate, then the situation will be dramatically different. In this case PS has been shown to be located preferentially at both the air and substrate interfaces. Studies are currently in progress to examine this case.

Increasing the total film thickness to $3L/4$, i.e., ~550–600 Å, produces the reflectivity profile shown in Figure 5. Again geometric effects cause the depression of the reflectivity at very low $k_{z,0}$. Above the critical $k_{z,0}$ the reflectivity decreases with a series of oscillations, which at large $k_{z,0}$ become quite regular. In fact, it is only the first maximum that shows evidence of a second frequency beating against the dominant frequency. Thus, it is apparent that a phase-separated, layered morphology is present. The solid line in the figure is the reflectivity calculated by using the simple bilayered scattering length density profile shown in the inset. This profile can be described by a 345-Å layer of d-PS on top of a 210-Å layer of PMMA. An oxide layer of ~20 Å is also evident. The width of the interface between the PS and PMMA layer is ~100 Å, much larger than that seen for the $L/4$ and $L/2$ cases and for the lamellar microdomain morphology in the bulk. The retention of the bilayered morphology mandates that the number of copolymer chains per unit area crossing the interface has increased and that the extension of the copolymer chains at the interface has increased. Despite the nearly 50% increase in the microdomain sizes over that found for the $L/2$ specimen and the corresponding stretching of the copolymer chains at the interface, a simple bilayered morphology is retained. An additional increase in the energy results from the increase in the number of segmental interactions between the d-PS and PMMA segments. These combined increases in the energy are, however, insufficient to force the copolymer to adopt a different morphology. These results clearly point to the dramatic amount a copolymer chain and the microdomain morphology can be perturbed by the imposition of the external constraints of the film thickness and the preferential interactions of the two blocks with different interfaces.

Finally, the reflectivity profile for the L-thick specimen, ~730 Å, is shown in Figure 6. In comparison to the profiles for the $L/4$, $L/2$, and $3L/4$-thick specimens, this reflectivity profile is more complex. Several different frequencies are evident in the data. Consequently, a multilayered morphology can be inferred by the appearance of the reflectivity profile. However, the XPS data place a severe constraint on any model that can be used to describe the reflectivity profile. It will be recalled that XPS measurements clearly showed that the volume fraction of d-PS at the air surface over the first ~75 Å in the film was 0.54. The scattering length density profile shown in the inset was used to calculate the solid line shown in Figure 6. Overall, the agreement between the calculated and measured reflectivity profiles is quite good although the calculated profile overestimates the shoulder occurring at $k_{z,0} \sim 0.01$ Å^{-1}. This could be improved by increasing the number of parameters in the scattering length density profile, but that did not seem justified at this point since the basic physics is captured in the scattering length density profile shown in the inset. This profile can be described by a mixed layer of d-PS and PMMA segments with an average scattering length density of 3.86×10^{-6} Å^{-2}. This corresponds to a volume fraction of d-PS of 0.54, in agreement with the XPS results. The thickness

Table III
Average Compositions

sample	$(\overline{b/V})$,[a] Å^{-2} × 10^6	ϕ_{PS}	deviation,[b] %
$L/4$	3.97	0.58	1.8
$L/2$	4.01	0.59	3.5
$3L/4$	4.17	0.62	8.8
L	4.14	0.62	8.8
$3L/2$	3.92	0.57	0

[a] $\overline{(b/V)} = \sum_i t_i(b/V)_i$, where t_i is the thickness of layer i with a scattering length density $(b/V)_i$. [b] Calculated from $[(\bar{\phi}_{PS} - \phi_{PS,A})/\phi_{PS,A}] \times 100$ where $\phi_{PS,A}$ is the volume fraction of PS in the copolymer based on the number of PS and PMMA segments in the copolymer. $\phi_{PS,A} = 0.57$.

of this layer is ~250 Å. This layer rests on a pure PS layer of ~313 Å separated by an interface with a width of ~200 Å. Underneath this d-PS layer is a 163-Å layer of PMMA with an interfacial width of 50 Å. Also seen is an oxide layer on the Si substrate with a thickness of ~15 Å. Thus, these data show that the extension of the chains seen in the $3L/4$-thick specimen does not continue as the film thickness is increased. This is, evidently, too costly energetically. It is also evident that the formation of islands on the surface of the film is too costly due to either the increase in the surface energy or the insufficient quantity of excess copolymer to form the islands. Thus, the copolymer initially forms a bilayer at the substrate comprised of a 163-Å layer of PMMA with a layer of d-PS that is larger than the 225 Å seen for the $L/2$ specimen. However, if a relaxed bilayer at the substrate is assumed comprising a thickness of 388 Å, the remaining 338-Å film of the copolymer is essentially in contact with a PS substrate. The copolymer is then in a situation where PS preferentially segregates to both the air interface and a PS substrate. Faced with this situation, the diblock copolymer does not microphase separate but, rather, remains phase mixed. This basically means that the energetic cost of mixing the d-PS and PMMA segments is less than the energy associated with placing PMMA at the air surface or adjacent to the PS layer and that associated with forming much smaller phases with PS at both the air interface and PS substrate. Thus, it appears from these results that if there is a preferential segregation of one block to both interfaces, then the constraint placed on the specimen by the film thickness, where the thickness is $L/2$ or less, is sufficient to cause an apparent elevation of the microphase-separation transition temperature. This forces a normally microphase-separated morphology into a phase-mixed state. As mentioned previously, this is being pursued further by using Au substrates that preferentially adsorb PS over PMMA.

As a test of the internal consistency of all the models that have been presented up to this point, the average composition of the film can be calculated. From the scattering length density profiles, the average scattering length density $(\overline{b/V})$ can be directly calculated. Since the scattering length densities of d-PS and PMMA are known and

$$\phi_{PS}(b/V)_{d\text{-}PS} + \phi_{PMMA}(b/V)_{PMMA} = (\overline{b/V}) \qquad (1)$$

then ϕ_{PS} can be easily obtained. For all the models used in the calculations, the value of ϕ_{PS} is shown in Table III. These values of ϕ_{PS} should be compared to the value of 0.57 obtained from the composition of the diblock copolymer. In reference to the composition of the diblock copolymer, the average composition calculated from the models is to within 9% of the ideal value. This agreement should be considered quite good and indicates that the models used to describe the reflectivity profiles are not unreasonable in terms of the average composition.

An alternative approach to the fitting of the reflectivity profiles would have been to use $(\overline{b/V})$ as an additional constraint on the fitting. While this is quite reasonable, such a constraint would have forced an overinterpretation of the reflectivity data in that shallow gradients extending into the PS or PMMA layers away from the interface could have been incorporated into the models. These could have been adjusted such that the proper $(\overline{b/V})$ was obtained, but it is not clear that other types of modifications to the models would have yielded as good fits to the data. Basically this reverts to the question of the nonunique nature of the fitting. Consequently, as stated before, the most simple model was used to describe the data. Anything more than this could not be distinguished by the reflectivity measurements. It is very clear, though, that the model calculations must yield a reasonable value of $(\overline{b/V})$ and, for the intent of this article, being to within 10% of the ideal value was considered quite reasonable. Thus, while the fine details of the models may not be absolutely correct, the models do capture the basic physics.

In summary, it has been shown that the constraints placed on a copolymer film by the thickness of the specimen can produce severe perturbations of the morphology. The perturbations are strongly influenced by the interactions of the blocks of the copolymer with the air interface and with the substrate. It is possible to induce variations in the extension of the chains at the interface and in the width of the interface separating the microphases. It is also possible to elevate the microphase-separation transition temperature and force a normally microphase-separated copolymer into a phase-mixed state. The results from the neutron reflectivity measurements have been found to be consistent with independent XPS, X-ray reflectivity, and ellipsometry measurements.

Acknowledgment. We thank D. C. Miller of the IBM Almaden Research Center for performing the X-ray photoelectron spectroscopy measurements. This work was partially supported by the Department of Energy, Office of Basic Energy Sciences, under Grant DE-FG03-88ER45375. Work at Argonne was supported by the U.S. Department of Energy, BES-Materials Sciences, under Contract W-31-109-Eng-30.

References and Notes

(1) See, for example: *Developments in Block Copolymers. 1*; Goodman, I., Ed.; Applied Science: New York, 1982.
(2) Molau, G. E. In *Block Copolymers*; Aggarval, S. L., Ed.; Plenum Press: New York, 1970.
(3) Hashimoto, T.; Fujiura, M.; Kawai, H. *Macromolecules* **1980**, *13*, 1660.
(4) Gallot, B. R. *Adv. Polym. Sci.* **1979**, *29*, 85.
(5) Thomas, E. L.; Alward, D. B.; Kinning, D. J.; Martin, D. C.; Handlin, D. L., Jr.; Fetters, L. J. *Macromolecules* **1986**, *19*, 2197.
(6) Hasegawa, H.; Tanaka, H.; Yamasaki, K.; Hashimoto, T. *Macromolecules*, in press.
(7) Bates, F. S.; Cohen, R. E.; Berney, C. V. *Macromolecules* **1982**, *15*, 589.
(8) Thomas, E. L.; Kinning, D. J.; Altward, D. B.; Henkee, C. S. *Macromolecules* **1987**, *20*, 2934.
(9) Meier, D. J. In *Block and Graft Copolymers*; Burke, J. J., Weiss, V., Eds.; Syracuse University Press: Syracuse, NY, 1982.
(10) Helfand, E.; Wasserman, Z. R. In *Developments in Block Copolymers. 1*; Goodman, I., Ed.; Applied Science: New York, 1982.
(11) Leibler, L. *Macromolecules* **1980**, *13*, 1602.
(12) Helfand, E. *Macromolecules* **1975**, *8*, 552.
(13) Helfand, E.; Wasserman, Z. R. *Macromolecules* **1976**, *9*, 879.
(14) Ohta, T.; Kawasaki, K. *Macromolecules* **1986**, *19*, 2621.
(15) Semenov, A. N. *Zh. Eksp. Teor. Fiz.* **1985**, *88*, 1242 (*Sov. Phys.–JETP* **1985**, *61*, 733).

(16) Anastasiadis, S. H.; Russell, T. P.; Satija, S. K.; Majkrzak, C. F. *Phys. Rev. Lett.* **1989**, *62*, 1852.
(17) Green, P. F.; Christensen, T. M.; Russell, T. P.; Jérôme, J. *J. Chem. Phys.* **1990**, *92*, 1478.
(18) Rastogi, A. K.; St. Pierre, L. E. *J. Colloid Interface Sci.* **1969**, *31*, 168.
(19) Thomas, H. R.; O'Malley, J. J. *Macromolecules* **1979**, *12*, 323.
(20) Schmitt, R. L.; Gardella, J. A., Jr.; Magill, J. H.; Salvati, I., Jr.; Chin, R. L. *Macromolecules* **1985**, *18*, 2675.
(21) Vanzo, E. *J. Polym. Sci., Polym. Chem. Ed.* **1966**, *4*, 1727.
(22) Bradford, E. B.; Vanzo, E. *J. Polym. Sci., Polym. Chem. Ed.* **1968**, *6*, 1661.
(23) Wittmann, J. C.; Lotz, B.; Candau, F.; Kovacs, A. J. *J. Polym. Sci., Polym. Phys. Ed.* **1982**, *20*, 1341.
(24) Hasegawa, H.; Hashimoto, T. *Macromolecules* **1985**, *18*, 589.
(25) Anastasiadis, S. H.; Russell, T. P.; Satija, S. K.; Majkzak, C. F. *J. Chem. Phys.* **1989**, *92*, 5677.
(26) Coulon, G.; Russell, T. P.; Deline, V. R.; Green, P. F. *Macromolecules* **1989**, *22*, 2581.
(27) Russell, T. P.; Coulon, G.; Deline, V. R.; Miller, D. C. *Macromolecules* **1989**, *22*, 4600.
(28) Coulon, G.; Aussere, D.; Russell, T. P. *J. Phys. (Paris)* **1990**, *51*, 777.
(29) Coulon, G.; Collin, B.; Aussere, D.; Chateney, D.; Russell, T. P. *J. Phys. (Paris)* **1990**, *51*, 2801.
(30) Henkee, C. S.; Thomas, E. L.; Fetters, L. J. *J. Mater. Sci.* **1988**, *23*, 1685.
(31) Green, P. F.; Christensen, T. M.; Russell, T. P. *Macromolecules* **1991**, *24*, 252.
(32) Lekner, J. *Theory of Reflectivity*; Nijhoff: Dordrecht, The Netherlands, 1987.
(33) Heavens, O. S. *Optical Properties of Thin Solid Films*; Butterworths: London, 1955.
(34) Born, M.; Wolf, E. *Principles of Optics*, 6th Ed.; Pergamon Press: Oxford, 1980.
(35) Werner, S. A.; Klein, A. G. *Neutron Scattering*; Skold, K., Price, D. C., Eds.; Academic Press: New York, 1986.
(36) Felcher, G. P.; Hilleke, R. O.; Crawford, R. K.; Haumann, J.; Kleb, R.; Ostrowski, G. *Rev. Sci. Instrum.* **1987**, *58*, 609.
(37) Russell, T. P. *Mater. Sci. Rep.* **1990**, *5*, 171.
(38) Green, P. F.; Russell, T. P.; Jerome, R.; Granville, M. *Macromolecules* **1988**, *21*, 3266.
(39) Bacon, G. F. *Neutron Diffraction*, 3rd ed.; Clarendon Press: Oxford, England, 1975.
(40) Optical microscopy measurements showed a single interference color indicative of the lack of islands or depressions on the film surface.
(41) Karim, A. Ph.D. Thesis, Northwestern University, 1990.

Registry No. P(d-S-*b*-MMA), 106911-77-7.